Ray tracing analysis of $CH_3NH_3PBI_3$-based perovskite solar cells: effects of various perovskite, ETL and HTL thicknesses

N. A. H. Rahime [a], A. Azis [a], M. Z. M. Yusoff [a,b,c,*], M. S. Yahya [d]
[a] *School of Physics and Material Studies, Faculty of Applied Sciences, Universiti Teknologi MARA, 40450 Shah Alam, Malaysia*
[b] *Institute for Biodiversity and Sustainable Development (IBSD), Universiti Teknologi MARA, 40450 Shah Alam, Malaysia*
[c] *Institute of Science (IOS), Universiti Teknologi MARA, 40450 Shah Alam, Malaysia*
[d] *Energy Storage Research Group, Faculty of Ocean Engineering Technology and Informatics, Universiti Malaysia Terengganu, 21030, Terengganu, Malaysia*

This study investigates how the thickness of the $CH_3NH_3PbI_3$ perovskite layer influences light absorption and the power conversion efficiency of the solar cell. The goal for this research is to identify the optimum values of perovskite nanocrystalline ($CH_3NH_3PbI_3$) thickness layer, to determine the ideal thickness of hole transport layer (HTL) and electron transport layer (ETL) to achieve maximum photocurrent density (J_{max}) and to investigate the relationship between the hole transport layer (HTL) and electron transport layer (ETL) thickness on perovskites solar cell performance. Wafer Ray Tracer calculator from PV Lighthouse simulation is used in this research to achievesthe objectives. The result shows the optimum thickness for the nanocrystalline perovskite layer, ETL of TiO_2 and HTL of Spiro-OMeTAD is 400nm, 40nm and 200nm respectively. In conclusion, the Wafer Ray Tracer calculator can do the modelling and analysis of nanocrystalline perovskite solar cells by varying their thickness.

(Received February 13, 2025, Accepted May 26, 2025)

Keywords: Solar; perovskite; $CH_3NH_3PbI_3$; Ray Tracing

1. Introduction

Perovskite solar cells have attracted significant attention in recent years due to their high-power conversion efficiencies and the potential for low-cost fabrication. This research regarding perovskite solar cells satisfied the second, third, and seventh SDG goals which are zero hunger, good health and world being and affordable and clean energy, respectively. Nanocrystalline is a hybrid (organic-inorganic) solar cell which gives the best performance of power conversion efficiency compared to organic or inorganic solar cells. Nanocrystalline is made of polycrystalline material which has the size of grains about 100 nm. The problem at hand involves understanding the relationship between the thickness of the perovskite layer and the overall performance of the solar cell. The perovskite solar cell structure consists of a metal electrode, a hole transport layer (HTL), perovskites, an electron transport layer (ETL), and transparent conducting oxide. Typically, there are two types of perovskite configurations, which are regular n-i-p planar and inverted p-i-n planar. In perovskite solar cells, the electron transport layer (ETL) is typically an n-type semiconductor, while the hole transport layer (HTL) is typically a p-type semiconductor. The type of architecture that has the highest efficiency is the n-i-p type. Thus, this study uses a regular n-i-p planar structure. Different compositions can have different band gaps, absorption properties, and charge transport characteristics, all of which have an impact on the efficiency of the solar cell. In this research, titanium Dioxide (TiO_2) was used as the ETL in perovskite solar cells due to its suitable band

[*] Corresponding author: mzmy83@gmail.com
https://doi.org/10.15251/JOBM.2025.172.99

alignment, high electron mobility, and stability [1], [2], [3]. Spiro-OMeTAD was used as HTL in perovskite solar cells because of its high hole mobility, stability, and easy processability.

Wafer Ray Tracer is a calculator used to figure out the photogenerated current density in a solar cell or test structure under a specified illumination spectrum. It can be used to evaluate or enhance a cell's or test structure's optical qualities. This calculator makes use of the OPAL2 concept, which enables accurate calculation of reflection, transmission, and thin film absorption at a single surface. Wafer Ray Tracer uses a modified version of the original Monte Carlo ray-tracing technique in combination with thin film optics. The techniques used in photon absorption by semiconductor nanocrystals, polarization-dependent, reflection, or transmission at interfaces, and photoluminescent reemission. In the requested wavelength range, the Wafer Optics Calculator calculates optical losses and photogeneration. The photon current density is determined by integrating over the wavelength after weighting the magnitudes by the photon flux in the user-defined spectrum. The short-circuit current that could be drawn from a flawless solar cell created from a wafer is equal to the photogenerated current in a wafer.

2. Experimental details

The Wafer Ray Tracer simulator from PV Lighthouse was used in this simulation. The wafer ray tracer is a simulation tool that uses ray tracing to evaluate a wafer's optics. It can be used to determine the optimal thickness of the perovskite layer in nanocrystalline perovskite solar cells. The wafer ray tracer can also be used to calculate the photogenerated current density in a solar cell or test structure under a specific illumination spectrum. The thickness of the nanocrystalline ($CH_3NH_3PbI_3$) perovskite solar cells, ETL and HTL varies in this study to observe the graph of reflection and absorption.

Table 1. The thickness for each solar cell layer.

Solar Cell Layer	Material	Thickness (nm)	References
Electron Transport Layer (ETL)	Titanium Oxide (TiO_2)	40 - 80	[4]
Absorber Layer	Perovskites Nanocrystalline ($CH_3NH_3PbI_3$)	100 - 500	[5]
Hole Transport Layer (HTL)	Spiro-OMeTAD	50 - 200	[6]

The simulation for a nanocrystalline ($CH_3NH_3PbI_3$) perovskite solar cell is done using the Wafer Ray Tracer (WRT) calculator. The spectrum used is sunlight at AM1.5G and is fixed for the whole simulation. This simulation is done using a range of thickness from 100nm-500nm with a scale of 100nm, and the suggested thickness is referred to in [5]. The ray tracing is performed to obtain the absorption and reflection graphs. After obtaining the optimum thickness of the nanocrystalline perovskite solar cell layer, its value is fixed for the simulation of HTL. The suggested thickness for HTL is in the range of 50nm-200nm with a scale of 50nm. In this simulation, four different thicknesses of HTL are stimulated using WRT. The previous steps are repeated, where the value of the nanocrystalline perovskite solar cell and HTL thickness are fixed once the optimum thickness is obtained by using WRT. There are five thicknesses of ETL in the range of 10nm-50nm with a scale of 10 nm, chosen for this simulation. The graph of absorption and reflection for various thicknesses of ETL is plotted. From the simulation, the value of photocurrent density can be obtained by using the formula (1):

$$J_{max} = q \int_{\lambda=400nm}^{\lambda=800nm} EQE(\lambda).S(\lambda)d\lambda \tag{1}$$

where q is the constant of electron charge, $1.6 \times 10^{-19}C$, and S is the standard spectral photon density of sunlight for AM1.5G. EQE stands for external quantum efficiency and can be calculated from IQE (internal quantum efficiency) multiplied by A (absorption). IQE is assumed to be IQE=1. The value of photocurrent density is obtained by integrating EQE with the solar spectrum at 1.5 AMG within the wavelength range of 400nm to 800nm. The range of 400nm – 800nm is chosen because it is the range in the solar radiation spectrum where invisible light occurs.

3. Results and discussion

3.1. Nanocrystalline ($CH_3NH_3PbI_3$) perovskite solar cell as absorber layer

For the absorber layer, the overall trend of the reflection graph from 400 nm to 500 nm remains unchanged and slowly decreases from 500 nm to 700 nm. It then rises drastically from 700 nm to 800 nm. At a thickness of 100 until 300 nm, the trend slowly decreases from 400 nm to 700 nm and rises from 700 nm to 800 nm. For a thickness of 400 nm, the trend fluctuates: it remains unchanged from 400 nm to 450 nm, slightly increases at 500 nm, then decreases until 600 nm. At a thickness of 500 nm, the trend also fluctuates. It shows a small increase from 400 nm to 600 nm, decreases at 650 nm, and starts increasing again at 700 nm. We suggest that the reflection of light may decrease as the thickness of the film increases due to a reduction in the refractive index difference between the perovskite film and the surrounding medium [4]. The absorption graph for the absorber layer shows the same trend for every thickness. The trend of the graph is a steady hold from the wavelength of 400 nm to 500 nm. A small change occurs at the 550 nm wavelength before it increases to 700 nm. At a wavelength of 750 nm, the graph falls to 800 nm. The absorber layer thickness is one of the parameters affecting the efficiency of solar cells and contributing to optimizing their performance [7], [8]. The electroluminescence performance of perovskite solar cells is frequently compromised at certain thicknesses due to photons emitted internally being trapped or reabsorbed [9]. We found that the absorption of light increases as the thickness of the nanocrystalline perovskite film increases. This is because there is more perovskite material available for light absorption.

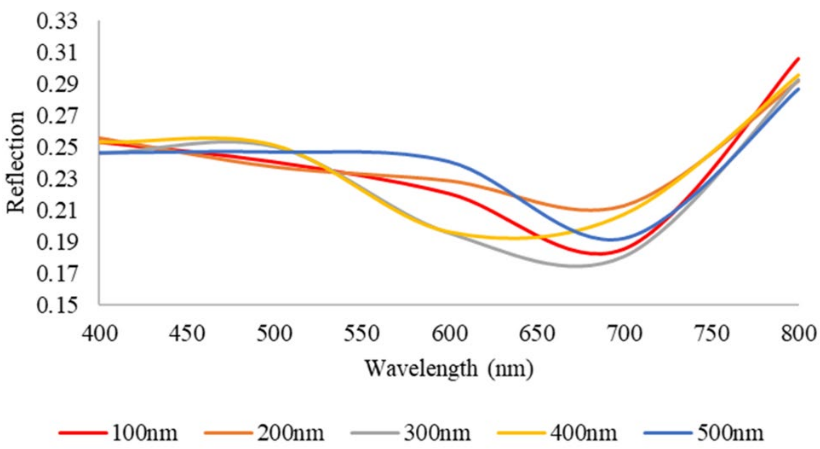

Fig. 1. Reflection graph for various nanocrystalline perovskite solar cell thickness.

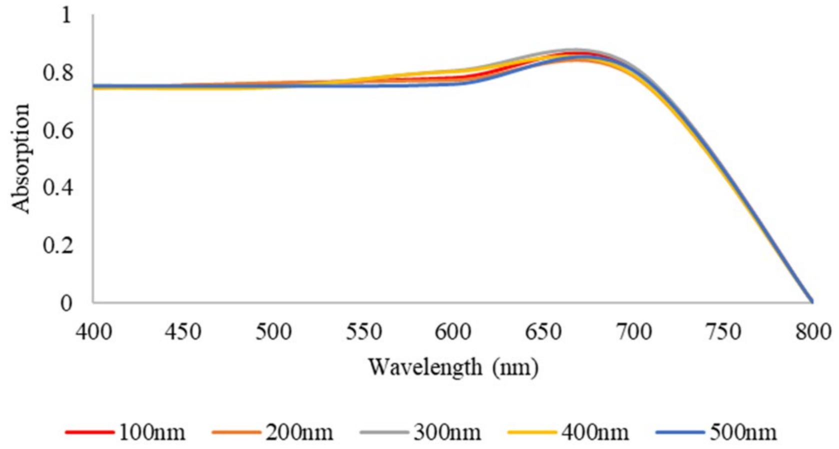

Fig. 2. Absorption graph for various thickness of nanocrystalline perovskite solar cell.

By integrating EQE with the AM1.5G solar spectrum at the wavelength range of 400 nm to 800 nm, the value of the photocurrent density of the absorber layer can be identified. From the calculation, the value of the photocurrent density of a nanocrystalline ($CH_3NH_3PbI_3$) perovskite solar cell is tabulated into Table 2. The data in the table shows the photocurrent density for various thicknesses of absorber layer. The J_{max} for 100 nm thickness is 0.1985 (mA/cm²). J_{max} stated at 200 nm thickness and 300 nm is 0.1972 (mA/cm²) and 0.982 (mA/cm²) respectively. The highest photocurrent density is shown at a thickness of 400 nm for 0.1994 (mA/cm²), which indicates the optimum thickness for the absorber layer. Lastly, the J_{max} for 500 nm thickness is 0.1973 (mA/cm²).

Table 2. The photocurrent density for various thicknesses of nanocrystalline ($CH_3NH_3PbI_3$) perovskite solar cell.

The Thickness of Nanocrystalline ($CH_3NH_3PbI_3$) Perovskite Solar Cell (nm)	Photocurrent Density (J_{max}) (mA/cm²)
100	0.1985
200	0.1972
300	0.1982
400	0.1994
500	0.1973

In this study, the 400 nm thickness of a nanocrystalline ($CH_3NH_3PbI_3$) perovskite solar cell was considered optimal due to reasons such as light absorption, charge carrier transport, and minimal defects. Perovskite materials are highly light-absorbing, with thicker layers absorbing more light. The perovskite layer, with a thickness of 400 nm, can efficiently capture a significant portion of incident sunlight, maximizing light absorption and promoting higher power conversion efficiency [10]. The perovskite layer, with a thickness of 400 nm, may provide an optimal pathway for efficient charge carrier transport, minimizing recombination losses and enabling higher efficiency. An increase in the thickness of the active layer beyond 400 nm can result in increased defects in the thin film [11]. Thus, the optimum thickness chosen for a nanocrystalline perovskite solar cell is 400 nm.

3.2. Hole transport layer (HTL) of Spiro-OMeTAD material

HTL thickness of 50 nm shows a fall from the wavelength of 400 nm to 550 nm. It remains unchanged from 600 nm to 650 nm and rises to 800 nm. The thickness of 100 nm shows small decreases at wavelengths of 400 nm to 500 nm, then falls to 650 nm. The trend suddenly increases at the wavelengths of 700 nm to 800 nm. The trend for thickness at 150 nm is different from the others as it increases from wavelengths of 400 nm to 500 nm before falling to 700 nm. The graph increases at 700 nm. Lastly, the trend of the graph for thickness at 200 nm is fluctuating. At the wavelengths of 400 nm to 500 nm, it shows a decreasing trend. At the wavelength of 500 nm, the graph is increasing, and a small decrease occurs at 600 nm to 700 nm. The trend is slowly increasing at 700 nm.

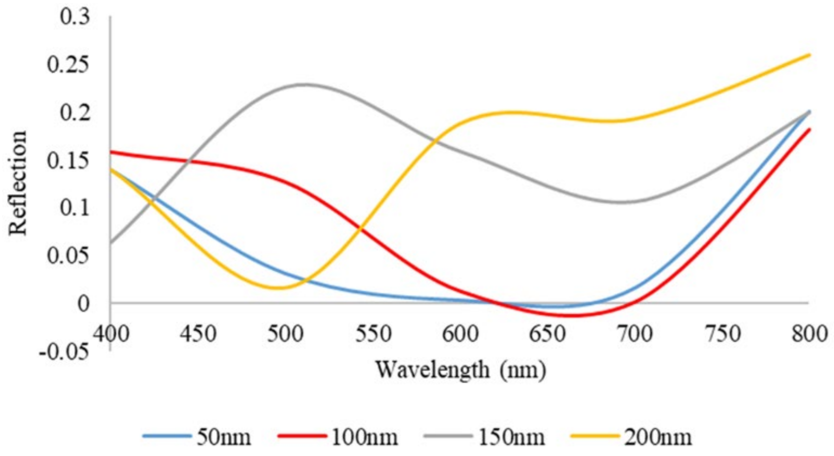

Fig. 3. Graph of reflection for various HTL thicknesses.

The absorption graph for various HTL thicknesses overall shows the same trend for four thicknesses at 50 nm, 100 nm, 150 nm, and 200 nm. At the wavelengths 400 nm to 450 nm, the four thicknesses show an increasing trend before a small decreasing trend at 450 nm. At the wavelengths of 500 nm to 700 nm, thicknesses at 50 nm, 100 nm, and 150 nm are steady except for 200 nm. At 200 nm, the absorption graph fluctuates in the range of 450 nm to 600 nm before steadily holding. The graph of reflection for all thicknesses slightly increases at 750 nm and then falls to 0 percentage of absorption at the wavelength of 800 nm.

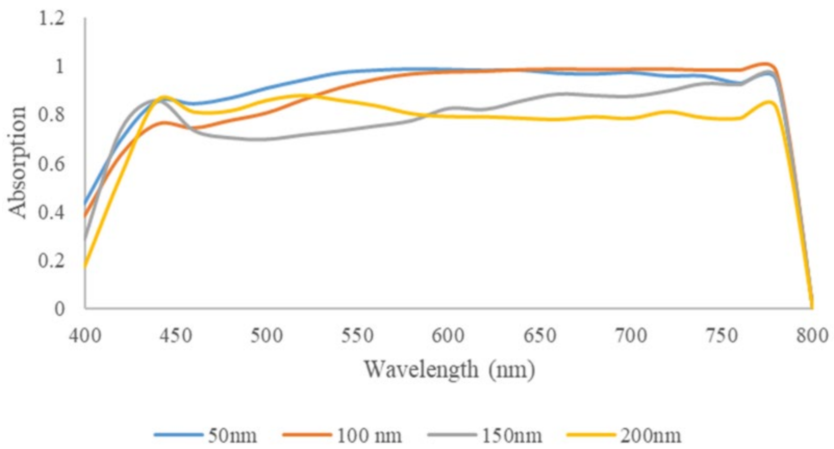

Fig. 4. Graph of absorption for various HTL Spito-OMeTAD thicknesses.

The photocurrent density can also determine the power conversion efficiency of a solar cell. By calculating J_{max} at the wavelength range of 400 nm to 800 nm, the value of the photocurrent density of the HTL Spiro-OMeTAD material can be identified. The data is tabulated in Table 3. At the thickness of 50 nm, the J_{max} obtained is 0.2356 mA/cm^2, also stated to be the highest J_{max} among the four thicknesses studied. The J_{max} at thickness 100 nm is the second highest, which is 0.2298 mA/cm^2 which is followed by 150 nm. The J_{max} calculated at 150 nm is 0.2053 mA/cm^2. The lowest J_{max} obtained is at 200 nm for 0.2007 mA/cm^2.

Table 3. The photocurrent density for various HTL (Spiro-OMeTAD) thicknesses.

The Thickness of HTL of Spiro-OMeTAD (nm)	Photocurrent Density (J_{max}) (mA/cm^2)
50	0.2356
100	0.2298
150	9.2053
200	0.2007

From the ray tracing simulation, the optimum thickness obtained for HTL of Spiro-OMeTAD material is 50 nm. The factors that are taken into consideration are charge transport efficiency, charge extraction, and light absorption and transmission. The HTL in solar cells is in charge of transporting holes (positive charge carriers) from the light-absorbing perovskite layer to the electrode. A study of the thickness of the hole transport layer (HTL) in perovskite solar cells discovered that a very thin HTL (50 nm) reduces the reproducibility and stability of the device because the counter electrode can pierce through the layer. A 50 nm thickness provides an optimal pathway for efficient hole transport, lowering recombination losses and improving charge collection efficiency. A 50 nm HTL could allow for more effective hole extraction from the perovskite layer, resulting in improved device performance. Thicker HTL layers may obstruct hole extraction, resulting in decreased efficiency. This result is supported by a previous study [12]; the thickness of the hole transport layer in perovskite solar cells was determined to be 50 nm, which reduces the reproducibility of device performance and stability because the counter electrode can pierce through the layer. Furthermore, a thicker HTL may reduce light transmission through the device, resulting in lower light absorption in the perovskite layer. A 50 nm HTL thickness could optimize overall light harvesting by balancing light absorption and transmission. To support the result obtained, Bag et al., (2020) stated that a very thin HTL (<50 nm) and a very thick HTL (>200) are not suitable for high efficiency. Inadequate thickness can cause recombination and leakage within the device [6]. More than 200 nm of thickness causes series resistance in the cell.

3.3. The electron transport layer of titanium dioxide (TiO_2)

The simulation using WRT for the thickness of ETL at 40 nm, 50 nm, 60 nm, and 80 nm has generated a graph of reflection and absorption. The overall graph of reflection for various ETL of TiO_2 material thicknesses shows the same trend. At the wavelengths of 400 nm to 500 nm, the graph trend shows a small decrease in the reflection of ETL for all thicknesses. The trend then starts to rise at a range of wavelengths from 500 nm to 600 nm before leveling off at 650 nm. In the range of 700 nm to 800 nm wavelengths, the graph drastically increases for all thicknesses of ETL.

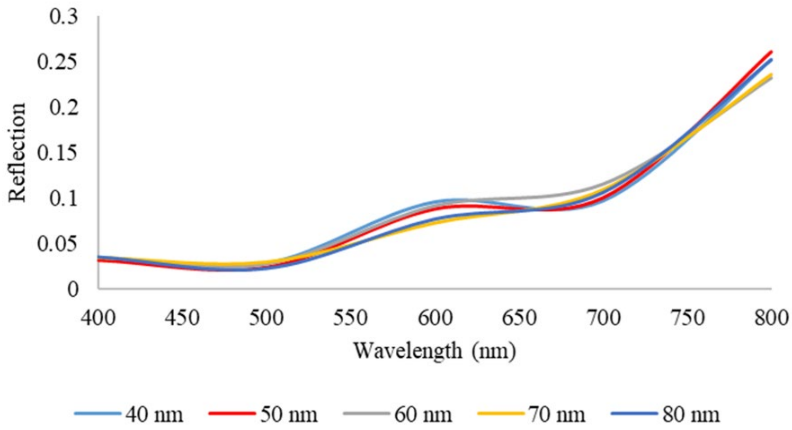

Fig. 5. Graph of reflection for various ETL thickness.

The graph of absorption for various thicknesses of ETL also shows the same trend for all thicknesses. Generally, the graph fluctuates. The graph started to increase at the wavelengths of 400 nm to 400 nm before decreasing in a small value to 450 nm. The graph steadily decreases with small changes but is constant in the range of wavelengths from 450 nm to 750 nm. The graph rises a small amount at 750 nm and falls drastically to a wavelength of 800 nm.

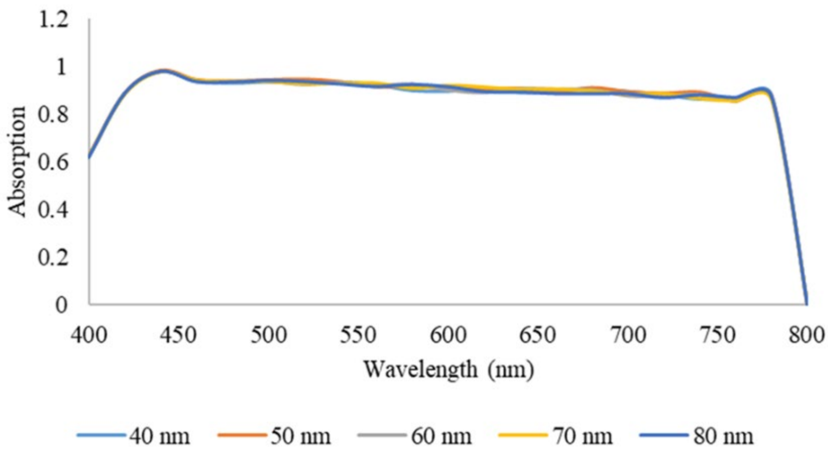

Fig. 6. Graph of absorption for various ETL thicknesses.

The same formula is used to calculate the photocurrent density for ETL of TiO_2 material. At a thickness of 40 nm, the J_{max} obtained is 0.2282 mA/cm^2. The thickness of ETL at 50 nm stated the highest J_{max} of 0.2288 mA/cm^2. The thickness at 60 nm and 80 nm obtained the same J_{max}, which is 0.2281 mA/cm^2. Lastly, the photocurrent density obtained at a thickness of 70 nm is 0.2283 mA/cm^2.

Table 4. The photocurrent density for various ETL (TiO_2) thicknesses.

The Thickness of ETL of TiO_2 (nm)	Photocurrent Density (J_{max}) (mA/cm^2)
40	0.2282
50	0.2288
60	0.2281
70	0.2283
80	0.2281

The reflection and absorption of TiO_2 in the ETL can have a significant impact on the photocurrent density of a perovskite solar cell. Understanding these effects is critical for optimizing the device's performance. The TiO_2 layer can act as a reflective layer, reflecting some incident light back instead of absorbing it from the perovskite layer. A study on ultrathin TiO_2 layers in solar energy conversion devices discovered that the TiO_2 ETL layer thickness should be greater than 20 nm to ensure uniformity and quality [13]. The TiO_2 ETL layer can absorb some of the incident light, especially in the near-ultraviolet spectrum. The TiO_2 layer's absorption of light can reduce the amount of light reaching the perovskite layer, lowering the photocurrent density. From this study, the optimum photocurrent density for ETL is at a thickness of 50 nm with 0.2288 mA/cm^2. The thickness of ETL can affect the photocurrent density due to factors such as charge transport, optical losses, light scattering, and absorption of light. The addition of a thin layer of TiO_2 ETL can result in a significant increase in the basic photoelectric parameters when compared to perovskite deposited directly on the substrate. This implies that an optimal thickness is required to facilitate efficient charge transport and increased photocurrent density. However, an overly thick TiO_2 layer can cause optical losses where some of the incident light is reflected or absorbed within the ETL and does not reach the perovskite layer. Optical losses reduce the number of photons available to form electron-hole pairs in the active layer, resulting in a lower photocurrent density. This explains why the photocurrent density decreases as the thickness of the ETL increases. Besides, the thicker TiO_2 layers within the ETL may scatter more light, increasing the likelihood of multiple light interactions and improving light absorption. Excessive scattering, on the other hand, may result in light escaping the TiO_2 layer, resulting in a lower photocurrent density. Last but not least, a thicker TiO_2 layer can absorb more incident light, increasing the number of photons converted into electron-hole pairs within the ETL. Thus, it leads to a higher photocurrent density. From the result of the photocurrent density calculation, the thicknesses of ETL at 40 nm and 60 nm shows the same value of photocurrent density. The difference in photocurrent density between the ETL TiO_2 thickness of 40 nm and 60 nm is about 0.0001, which is a very small difference. According to the previous study [14], even minor variations in solar cell collection efficiency can affect the final power output. Even minor variations in high-efficiency solar cells can affect the final power output. However, in lower-efficiency cells, this difference may have little practical impact. This case is also supported by Mahmoud et al. (2023) [15]. The higher photocurrent density indicates that more photons are converted into electrical current, which results in a higher power output and efficiency [16]. Apart from that, the thickness of each layer is also considered one of the aspects leading to improved efficiency [17]. Hence, in this study, the thickness of the absorber layer, ETL, and HTL varied to identify the optimum photocurrent density.

4. Conclusion

In conclusion, the thickness of the absorber layer, hole transport layer (HTL), and electron transport layer (ETL) in perovskite solar cells plays a crucial role in determining the overall device performance. The optical properties, such as absorption and reflection, are influenced by the thickness of these layers and directly impact the photocurrent density, which is a key determinant of the solar cell's efficiency. For the absorber layer, the optimum thickness of the absorber layer is determined to be 400nm, providing efficient light absorption and minimal defects. For the HTL of Spiro-OMeTAD material, the reflection graph shows 50nm being the optimal thickness. This thickness allows for efficient hole transport and charge collection, promoting high device performance. For the ETL of TiO_2 material, the optimal thickness for ETL is determined to be 50nm, providing a balance between charge transport efficiency and light absorption. In summary, the results suggest that optimizing the thickness of each layer in the perovskite solar cell is crucial to achieve the highest efficiency. The simulation and calculation data support the conclusions drawn from previous research and validate the importance of precise layer thicknesses in perovskite solar cell design.

Acknowledgments

The support from Universiti Teknologi Mara, Shah Alam is also gratefully acknowledged.

References

[1] Prochowicz, D., Tavakoli, M. M., Wolska-Pietkiewicz, M., Jędrzejewska, M., Trivedi, S., Kumar, M., Zakeeruddin, S. M., Lewiński, J., Graetzel, M., Yadav, P. (2020, February), Solar Energy, 197, 50-57; https://doi.org/10.1016/j.solener.2019.12.070

[2] Hu, W., Yang, S., Yang, S. (2020, February), Trends in Chemistry, 2(2), 148-162; https://doi.org/10.1016/j.trechm.2019.11.002

[3] Chen, D., Su, A., Li, X., Pang, S., Zhu, W., Xi, H., Chang, J., Zhang, J., Zhang, C., Hao, Y. (2019, August), Solar Energy, 188, 239-246; https://doi.org/10.1016/j.solener.2019.06.016

[4] Sławek, A., Starowicz, Z., Lipiński, M. (2021, June 14), Materials, 14(12), 3295; https://doi.org/10.3390/ma14123295

[5] Hima, A., Lakhdar, N., Benhaoua, B., Saadoune, A., Kemerchou, I., Rogti, F. (2019, May), Superlattices and Microstructures, 129, 240-246; https://doi.org/10.1016/j.spmi.2019.04.007

[6] Bag, A., Radhakrishnan, R., Nekovei, R., Jeyakumar, R. (2020, January), Solar Energy, 196, 177-182; https://doi.org/10.1016/j.solener.2019.12.014

[7] Shahverdi, N., Yaghoubi, M., Goodarzi, M., Soleamani, A. (2019, September), Solar Energy, 189, 111-119; https://doi.org/10.1016/j.solener.2019.07.040

[8] Iakobson, O. D., Gribkova, O. L., Tameev, A. R., Nunzi, J. M. (2021, March 2), Scientific Reports, 11(1); https://doi.org/10.1038/s41598-021-84452-x

[9] Rai, M., Wong, L. H., Etgar, L. (2020, September 7), The Journal of Physical Chemistry Letters, 11(19), 8189-8194; https://doi.org/10.1021/acs.jpclett.0c02363

[10] Umar, A., Sadanand, Singh, P. K., Dwivedi, D. K., Algadi, H., Ibrahim, A. A., Alhammai, M. A. M., Baskoutas, S. (2022, December 12), Micromachines, 13(12), 2201; https://doi.org/10.3390/mi13122201

[11] Danladi, E., Dogo, D. S., Udeh, S. M., Uloko, F. O., Salawu, A. O. (2021, December 10). Recent Advances in Modeling of Perovskite Solar Cells Using SCAPS-1D: Effect of Absorber and ETM Thickness. 4, 4, 5-17; https://doi.org/10.26565/2312-4334-2021-4-01

[12] Kim, G. W., Shinde, D. V., Park, T. (2015), RSC Advances, 5(120), 99356-99360; https://doi.org/10.1039/C5RA18648J

[13] Zhou, C., Xi, Z., Stacchiola, D. J., Liu, M. (2022, March 31), Energy Science & Engineering, 10(5), 1614-1629; https://doi.org/10.1002/ese3.1142

[14] Kinsey, G. S. (2021, March), Solar Energy, 217, 49-57; https://doi.org/10.1016/j.solener.2021.01.024

[15] Mahmoud et al., 2023. Mahmoud, K. H., Alsubaie, A. S., Anwer, A. H., Ansari, M. Z. (2023, May 27), Micromachines, 14(6), 1127; https://doi.org/10.3390/mi14061127

[16] Ha, D., Yoon, Y., Park, I. J., Cantu, L. T., Martinez, A., Zhitenev, N. (2023, June 7), The Journal of Physical Chemistry C, 127(24), 11429-11437; https://doi.org/10.1021/acs.jpcc.3c00239

[17] Jeong, S. H., Park, J., Han, T. H., Zhang, F., Zhu, K., Kim, J. S., Park, M. H., Reese, M. O., Yoo, S., Lee, T. W. (2020, June), Joule, 4(6), 1206-1235; https://doi.org/10.1016/j.joule.2020.04.007